Hindawi Publishing Corporation
International Journal of Photoenergy
Volume 2014, Article ID 356365, 10 pages
http://dx.doi.org/10.1155/2014/356365

Research Article

Photoelectrocatalytic Degradation of Humic Acids Using Codoped TiO_2 Film Electrodes under Visible Light

Xiao Zhou,[1] Yongxin Zheng,[1] Dan Liu,[1] and Shaoqi Zhou[1,2,3,4]

[1] *College of Environment and Energy, South China University of Technology, Guangzhou 510640, China*
[2] *State Key Laboratory of Subtropical Building Science, South China University of Technology, Guangzhou 510641, China*
[3] *Key Laboratory of Environmental Protection and Eco-Remediation of Guangdong Regular Higher Education Institutions, South China University of Technology, Guangzhou Higher Education Mega Center, Guangzhou 510006, China*
[4] *Guizhou Academy of Sciences, Shanxi Road 1, Guiyang 550001, China*

Correspondence should be addressed to Shaoqi Zhou; fesqzhou@scut.edu.cn

Received 19 August 2013; Revised 18 October 2013; Accepted 18 October 2013; Published 13 February 2014

Academic Editor: Tian-Yi Ma

Cu/N codoped TiO_2 films on Ti substrates were successfully prepared by electrochemical method with the goal of enhancing the photoelectrocatalytic activity under visible light. The morphology and composition of the Cu/N codoped films were characterized using field emission scanning electron microscopy (FESEM), X-ray diffraction (XRD), energy dispersive X-ray (EDX), and UV-Vis diffusion reflection spectroscopy (UV-Vis DRS). The photocatalytic activities of the Cu/N codoped TiO_2 films were evaluated by the degradation of humic acid. The visible light photocatalytic degradation of humic acid (HA) was tested and Cu/N codoped TiO_2 films showed the highest degradation efficiency up to 41.5% after 210 minutes of treatment. It showed that Cu^{2+} and NH_4^+ codoped TiO_2 film significantly improved the photocatalytic efficiency under the visible light. When +5.0 V anodic bias potential and visible light were simultaneously applied, the degradation efficiency of HA over the Cu/N codoped TiO_2 films significantly improved to 93.5% after 210 minutes of treatment.

1. Introduction

Humic acid (HA) is the main fraction of the humic substances existing in fresh water sources and creating problems in treatment operations. Consequently, it is the primary target of water treatment process although not considered as a pollutant. The HA is a complex mixture of organic compounds, which is derived from the decomposition of plants and animal material [1–3]. Humic acid has been reported to bring about many negative effects in drinking water, including undesirable color and taste, absorption and concentration of organic pollutants, and biochemical decomposition. Moreover, when water is treated with chlorine for sterilization, humic acid could react with chlorine by a combination of substitution and oxidation mechanisms forming potentially carcinogenic organic compounds [1, 4, 5]; this has been a problem in past drinking water treatment. Increased concern is focused on the potential toxicity of humic acid and its precursors. Hence, the degradation techniques of humic acid need to be established.

In common water treatment processes, the removal of humic acid has been accomplished by physical separation, such as adsorption of activity carbon, precipitation and flocculation, ion exchange [4], and transfer of pollutants from one phase to another or concentrating them in one phase, without actually eliminating them, which is the main disadvantage associated with these techniques. Novel methods such as the Fenton process, ozonation, and electrochemical and photochemical technologies have been developed to decompose pollutants. Titanium dioxide (TiO_2) electrodes have been widely utilized as a photocatalytic material technology with applications in many fields such as environmental purification and decomposition of carbonic acid gases and solar cell, especially in the decomposition of recalcitrant organic pollutants [6–10]. In the last decades, it has been demonstrated that titanium dioxide (TiO_2) photocatalysis is one of the suitable advanced oxidation processes' (AOPs) techniques for the decomposition of refractory HA because of its excellent photostability, relatively low cost, nontoxicity,

and its ability to photooxidatively destroy most refractory pollutants [11, 12].

However, TiO_2 has three major limiting factors. The first is the low separation rate of photoinduced electron-hole pairs. Second, TiO_2 has low utilization efficiency of visible light because of its large band gap of 3.2 eV. UV light constitutes only a small fraction (5%) of the solar spectrum [13]. The last causes difficulty in separating suspended TiO_2 particles from the water; simultaneously, the water will be contaminated by the TiO_2 particles if they are not completely separated from water. These shortcomings hold back the TiO_2 application in water treatment. Nevertheless, extending the absorbance of TiO_2 to visible light and improving the photocatalytic efficiency of TiO_2 have the most important prospects.

For the first and the second problems, in order to reduce the high recombination rate of photoexcited electron-holes and utilize sunlight, a variety of methods, such as metal and nonmetal doping [14, 15], composites with the other semiconductors [16], dye sensitization [17], and surface modification [18], have been extensively applied. Among such methods, metal and nonmetal doping has been demonstrated to be an effective approach, having been widely studied in literature [14]. In particular, much effort has been made to enhance the visible light photoresponse of TiO_2 via doping main group elements including carbon, nitrogen, and sulfur [20–22] and transition metal elements such as W^{6+}, Fe^{3+}, Zr^{4+}, V^{5+}, and Mo^{6+} [23–27]. These compounds absorb visible light. The preceding findings are supported by the results of theoretical calculations using full potential linearized augmented plane wave formalism (F-LAPW method). Metal ions doped into the TiO_2 crystal lattice create a narrow energy band inside the TiO_2 band gap; as a result, photoinduced electrons can be easily activated and the photoresponse wavelength can be expanded to visible region. This can depend on the ion location in the host lattice and characteristics of the metal ions in question [28]. Nonmetal ions doping into the TiO_2 lattice can replace some of the oxygen vacancies, reducing the energy band gap and extending photoactive region. It should also be noted that dopants such as N are incorporated as anions and replaced by oxygen in the TiO_2 lattice. The N doping not only decreases the band gap, but also hinders the growth of crystalline particles; the resulting small size can facilitate the separation of charge carrier [23].

To solve the third problem, the immobilization of TiO_2 on various supports such as glass, ceramics, and zeolite remains one of the prerequisites to obtain an effective catalyst because this is a technological requirement to avoid the separation/filtration step. Different supports and different immobilization techniques for TiO_2 photocatalysts including thermal oxidation of titanium, anodic oxidation, and sputtering have been previously investigated. Immobilization of TiO_2 onto conducting substrate enables the application of electrochemistry techniques.

A novel method such as anodic oxidation method has been recently developed. The anodic oxidation method is a simple, cost-effective, and straightforward method to prepare highly ordered TiO_2 nanofilms on Ti substrate [29, 30], a process which allows the in-situ preparation of TiO_2 film electrodes. In this anodic oxidation process, using a pretreated Ti substrate as an anode and a platinum foil or other materials as the cathode, both units are placed in the electrolyte solution, and then a constant voltage is applied for a determined time. Oxidizing metallic titanium to directly create TiO_2 films provides a much stronger adhesion of the oxide to the substrate, a behavior which overcomes adherence problem [31, 32], therefore improving substrate stability of photocatalytic devices in flowing water and reducing resistance to electron transfer and the recombination of photogenerated electron transfer.

Vinodgopal et al. [33] published a paper in 1993 on TiO_2 thin film electrode degrading 4-chlorophenol efficiently under UV lamps. Subsequently, an efficient technique named photoelectrocatalysis (PEC) was proposed. In a sole photocatalysis process, the surface area of the catalyst in the film contacting pollutant molecules is reduced after TiO_2 powder is transformed to film; consequently, the photocatalytic degradation efficiency over TiO_2 film is usually lower than over TiO_2 powder. The difference of degradation efficiency between Degussa P25 powders and TiO_2 thin film could be 80% under the same degradation conditions [34]. So, to improve the degradation efficiency, photoelectrocatalytic degradation of pollutants has been developed by applying an external bias potential to various TiO_2 films [35–37]. The photoelectrocatalytic technique combines both electrolytic and photocatalytic processes. In the PEC process, the applied external potential is the key factor, and the separation of electron-hole pairs (e^-_{CB}/h^+_{VB}) is promoted by electron transfer via the control of an external circuit, significantly improving the performance of photocatalytic (PC) efficiency. The basic process of photocatalysis consists of ejecting an electron from the valence band (VB) to the conduction band (CB) of the TiO_2, thereby creating an "h^+" hole in the valence band. This is due to the solar irradiation of TiO_2 with an energy equal or superior to the band gap (3.2 eV). These charge carriers (e^-/h^+) can migrate to the surface of the catalyst, where they are then available to undergo redox reaction with substrates [38]:

$$TiO_2 + h\nu \longrightarrow e^-_{CB} + h^+_{VB} \quad (1)$$

This is followed by the formation of extremely reactive radical $OH^\bullet$ at the TiO_2 surface and/or a direct oxidation of the polluting species (R). The redox potential of $OH^\bullet/H_2O$ is 2.81V. Therefore, pollutants in wastewater can be degraded directly on the surface of the TiO_2 or indirectly by reacting with hydroxyl radicals [39]. The photogenerated hole in the valence bond can react with absorbed water molecular to form oxidative species such as $OH^\bullet$ which subsequently attack the pollutant:

$$\begin{aligned} h^+_{VB} + H_2O &\longrightarrow OH^\bullet + H^+ \\ h^+_{VB} + OH^- &\longrightarrow OH^\bullet_{ads} \\ h^+_{VB} + R_{ads} &\longrightarrow R^+ \end{aligned} \quad (2)$$

The electrons ejected to the conduction band can either react with electron acceptors such as adsorbed oxygen (O_2)

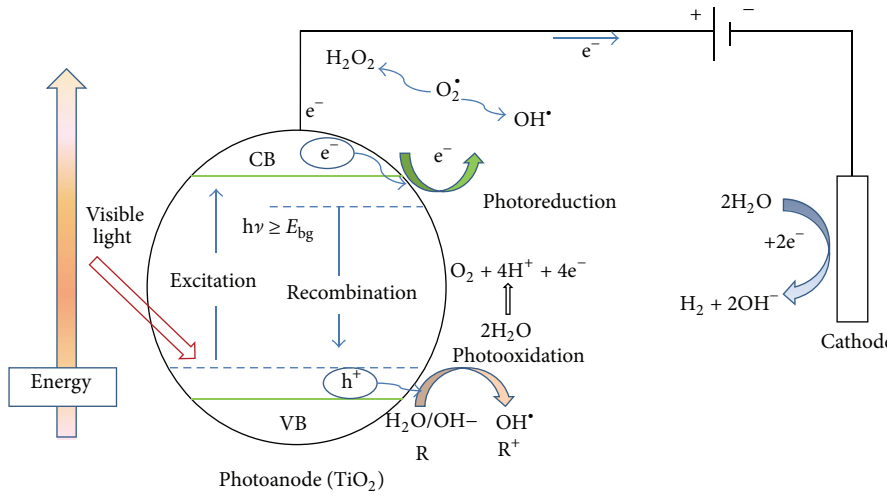

Figure 1: Mechanism of photoelectrocatalytic process using TiO_2 photocatalyst and the reactions that occur at the surface.

to form superoxide radicals (3) or react with adsorbed water molecule (H_2O) to form oxidative species such as hydroxyl radicals:

$$e^-_{CB} + O_2 \longrightarrow O_2^{\bullet -} \quad (3)$$

The photogenerated electrons (e^-) reduce the recombination rate of the photogenerated electron-hole pairs and enhance the photocatalytic activity [40]. The lifetime of the pairs (e^-_{CB}/h^+_{VB}) is a few nanoseconds. Without electron donors or acceptors these electron-hole pairs can recombine to release heat or migrate to the surface of the TiO_2 and react with species that have been adsorbed there:

$$e^-_{CB} + h^+_{VB} \longrightarrow \text{heat} \quad (4)$$

Figure 1 shows the general mechanism of the photoelectrocatalytic process and the main reaction that occurs at the surface of TiO_2 [41]. According to the literature [41], when a positive bias is applied to the Ti/TiO_2 photoanode, the generated electrons can be transferred into the external circuit instead of the oxygen molecule. As a result, the photogenerated hole or $OH^\bullet$ will be left at the surface of the TiO_2 electrode. Therefore, the rate of photogenerated electron-hole recombination is limited while a possibility exists to improve the efficiency of oxidation at the semiconductor-electrolyte interface.

Whether in the PC or in the PEC process, the degradation rate of refractory pollutants depends on the activity of the titania film electrodes. In recent years, photoelectrocatalytic degradation of organic pollutants has attracted much interest under visible light [42–44].

Therefore, to investigate the effect of various TiO_2 films electrodes, in this work, we successfully prepared Cu/N codoped TiO_2 films by the anodic oxidation process to study the photoelectrocatalytic degradation of humic acid (HA) under visible light illumination. The surface morphology, crystallization, and photoelectrochemical characteristics of the hybrid films were investigated with various techniques, including field emission scanning electron microscopy (FESEM), energy dispersive X-ray (EDX), X-ray diffraction (XRD), UV-Vis diffusion reflection spectroscopy (UV-Vis DRS), UV-Vis spectroscopy, and voltammetry. The photoelectrocatalytic activity of these samples was evaluated on the basis of the degradation of humic acid (HA) in aqueous solution under visible light irradiation. Using such Cu/N TiO_2 films, the visible light photoelectrocatalytic degradation of HA was also studied in detail by changing the initial concentration affecting the degradation process. The Cu-N TiO_2 samples showed better photocatalytic activity with required degradation of humic acid (HA) than the TiO_2 films in visible light regions.

2. Materials and Methods

2.1. Materials. Titanium sheets (0.2 mm × 50 mm × 50 mm, 99.6% purity) were polished by metallographic abrasive paper and then degreased by sonicating process in acetone, isopropanol, and methanol. After rinsing with water, the materials were air-dried. Graphite electrodes were procured from Guangzhou Jinlong Technology Co., Ltd. Acetone, isopropanol, methanol, HF, HNO_3, $Cu(NO_3)_2$, NH_4Cl, and the abovementioned chemicals and solvents were of analytical grade and used without further purification. Commercial humic acid (CAS no. 308067-45-0) was purchased from Shanghai, China, and was used as received. The chemical components of HA indicated that the H/C atomic ratio and the O/C atomic ratio were 0.956 and 0.412, respectively. HA was dissolved in 0.1 M sodium hydroxide solution (NaOH, CAS no. 1310-73-2) and then separated by 0.45 μm membrane. The filtrate was diluted to a desired concentration ranging from 10 to 60 mg/L. Water used in all experiments was purified using a Milli-Q Plus 185 water purification system (Millipore, Bedford, MA) with a resistivity higher than 18 MΩ cm.

2.2. Preparation of TiO_2/Ti Electrode. The anodic oxidation was accomplished with a 33 V DC-power source using titanium sheet as anode and graphite as cathode. The distance

between two electrodes was set at 5 cm in all experiments. The electrolyte contained 0.01 M HF and 0.1 M HNO_3. The anodic oxidation was carried out under 20 V for 30 min. After electrolysis, the titanium sheet was rinsed with water and then air-dried.

2.3. Preparation of Cu/N TiO_2/Ti Film Electrode. The as-prepared TiO_2 electrode (on Ti sheet) was used as cathode and graphite as anode. The electrolyte was a mixture of different volumes of 0.2 M $Cu(NO_3)_2$ and 0.2 M NH_4Cl, and the molar ratio of $Cu^{2+}/NH_4{}^+$ was adjusted to 1 : 1, 1 : 2, 1 : 3; 2 : 1, 2 : 2, 2 : 3; and 3 : 1, 3 : 2, 3 : 3, respectively. The distance between two electrodes was kept at 5 cm. The entire electrochemical process was performed at 5 V for 1 h. Finally, the titanium sheet with Cu/N codoped TiO_2 surface was taken out and rinsed with water and then air-dried.

2.4. Calcination. Cu/N codoped TiO_2 and nondoped TiO_2 electrodes were calcined under air for 2 hours at the temperature of 500°C. To indicate the ratio of $Cu^{2+}/NH_4{}^+$ in electrolyte and calcination temperature, codoped samples are expressed as the form of Cu_1N_1/TiO_2, Cu_1N_2/TiO_2, Cu_1N_3/TiO_2, and so forth, while pure TiO_2 electrodes are expressed as TiO_2.

2.5. Photoelectrocatalytic Activity Measurements. The photoelectrocatalytic activity efficiencies for the prepared samples were tested by degradation of humic acid in aqueous suspension. The photoelectrocatalytic oxidation experiments were conducted in a glass beaker. During these experiments, different plate anode materials were tested: Cu/N TiO_2/Ti and graphite plates used as active anode surface during electrolysis. The electrodes were dipped into the beaker containing 0.6 L humic acid as working volume. A 50 W tungsten halogen lamp (EXZ MR16 SP, GE, USA) was used as visible light resource. The light intensity was 80.1 Mw cm^{-2} (380 nm~780 nm) measured by SpectraScan Spectroradiometers (PR-705, Photo Research, USA). The photoelectrocatalytic oxidation was carried out at a constant current using a digital DC power supply. The sample solution was agitated by a magnetic stirrer (Figure 2). Magnetic stirring at a slow speed was constantly maintained along with the reaction. The concentration of humic acid was analyzed at the maximum absorption wavelength of HA at 254 nm with a UV-Vis spectrometer (Unico UV-2800A, China).

2.6. Instruments and Analytical Methods. UV-Vis diffuse reflectance spectra were recorded on a Shimadzu 2550 UV-Vis spectrophotometer between 200 and 800 nm with $BaSO_4$ as the background. The XRD phase detection and analysis of the crystal structure of prepared products were recorded by a Dmax-rA powder diffractometer (Bruker D8 ADVANCE, Germany), with Cu Kα as a radiation and a step width of $2\theta = 0.02^\circ$, with 2θ ranging from 20 to 60. The morphological features of the prepared products were assessed using a LEO, 1530 Vp field-emission scanning electron microscope (FESEM) at 15 kV. SEM samples were sputter-coated with about 20 nm Au using a Polaron Sputter Coater system.

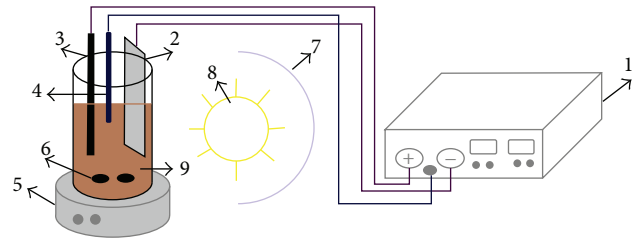

Figure 2: The electrochemical reactor and instrumentation. (1) DC power source, (2) Cu/N TiO_2/Ti anode, (3) graphite cathode, (4) reference electrode, (5) magnetic stirrer, (6) magnetic bar stirrer, (7) aluminum foil, (8) tungsten lamp, and (9) sample solution.

The SEM-EDX analysis was performed by a High Vacuum Tungsten Filament SEM (Hitachi S-3700N, Japan).

During the experiments, HA samples were periodically collected for analysis. No reactants or supporting electrolyte were added to the humic acid prior to the experiments. The UV-HA method was used for the measurement of HA concentration [45]. Specific UV absorbance of filtered samples was monitored at 254 nm with UV-Vis spectrophotometer (Unico UV-2800A, China), which was used to represent aromatic moieties. Additionally, UV-Vis spectrum was recorded from 200 to 600 nm. The samples were irradiated for 210 minutes. For absorbance measurement, 10 mL of sample was taken out from the reactor at given time intervals. All experiments were repeated at least two times, while reproducibility of the experiments was within 5%.

3. Results and Discussion

3.1. X-Ray Diffraction Analysis. X-ray diffraction patterns of TiO_2 film and the Cu/N codoped TiO_2 films calcinated at 500°C for 2 h are shown in Figure 3. During the process of annealing, a crystalline phase of TiO_2 was formed. The crystalline structures of the oxide films were dependent on the type of electrolyte that was used. Mixed crystalline structure consisting of anatase and rutile TiO_2 was observed for the Cu/N codoped TiO_2 groups.

Anatase phase of the TiO_2 crystal structure could be interpreted from XRD patterns for TiO_2 and Cu/N codoped TiO_2 films, where anatase characteristic peaks are mainly crystallized to 2θ values of 25.5° (101), 37.9° (004), 48.045° (200), and 54.1° (105), respectively. Small rutile peaks were also observed at 27.4° (110) and 36.1° (101). At the temperature of 500°C, anatase phase was formed. The rutile phase began to appear when the annealing temperature was increased to 600°C. For Cu/N codoped TiO_2 films, obvious rutile peaks emerged when calcined at 500°C. It seems that Cu/N codoping is helpful for the crystalline phase transition from anatase TiO_2 to rutile TiO_2. Both anatase and rutile peak intensities increased slightly after calcination as has been reported before [46, 47]. Many studies have demonstrated that the mixture of anatase and rutile TiO_2 has greater degradation efficiency than either anatase or rutile TiO_2 alone. So the Cu/N codoped TiO_2 films in this paper can improve the PEC degradation efficiency. No peaks for CuO were observed for the low Cu doping

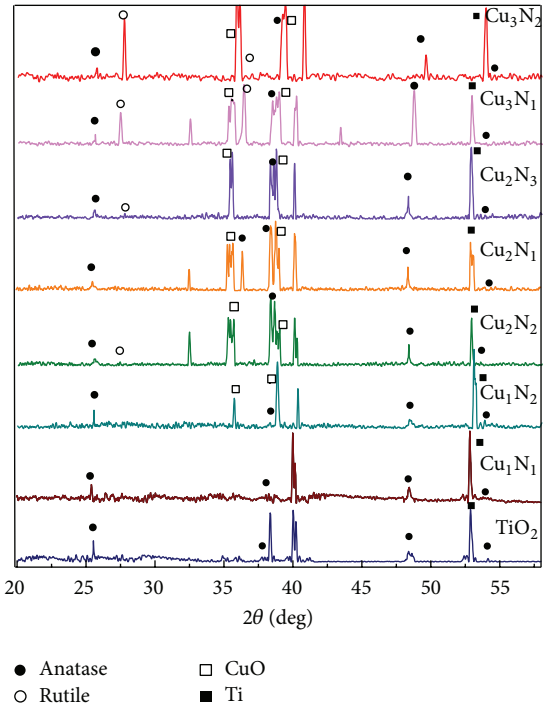

FIGURE 3: XRD patterns of TiO_2 and Cu/N codoped TiO_2 films with different Cu^{2+}/NH_4^+ molar ratios and annealed at 500°C.

samples. This was due to the low amount of Cu present. The diffraction peak intensities at $2\theta = 35.5^\circ$ and 38.7°, which were assigned to CuO (002 or 111) and CuO (111) [48], respectively, were observed for the samples of Cu_2N_x or Cu_3N_x, and their intensities increased with an increase in the Cu content. No nitrogen-derived peaks were detected, presumably due to the fact that content of N doping was very low.

3.2. UV-Vis Diffuse Reflection Spectroscopic Analysis. Figure 4(a) shows UV-Vis DRS spectra for Ti, TiO_2-500, and codoped TiO_2-500 plate electrode and Figure 4(b) shows the corresponding plot of transformed Kubelka-Munk versus energy of light for TiO_2-500 and codoped TiO_2-500. It can be seen that pure TiO_2 film absorbs UV light at a wavelength less than 400 nm. While the TiO_2 film is doped with Cu^{2+} and NH_4^+, there is about 40 nm red shift of the band edge for Cu/N codoped thin film. In addition, the absorption intensity in visible light regions is increased, suggesting an improved photocatalytic activity within the visible light range (see next). On the other hand, the absorption in the UV light range decreased slightly. Cu_1N_3 and Cu_1N_2 codoped nanofilms with different Cu^{2+}/NH_4^+ molar ratios calcined at 500°C exhibited more or less similar red shift of the band edge and also reduced reflection intensity when compared with the pure TiO_2 nanofilm. The red shift can be attributed to the fact that when TiO_2 is doped with copper, Cu^{2+} species can form Cu-O-Ti bond with Ti^{4+} and then the photoinduced electrons can be effectively trapped by Cu^{2+} species. Furthermore, some Cu^{2+} species are deposited on the surface of TiO_2 films, a condition which inhibits the absorption of visible light [48, 49].

The band gaps were estimated by application of the following equation:

$$(\alpha h\nu) = A\ (h\nu - E_g)^n, \tag{5}$$

where α, E_g, h, ν, n, and A are absorption coefficients, the band gap (eV), Planck's constant (6.6260×10^{-34}), frequency of light (s^{-1}), a number characterizing transition (for TiO_2, $n = 1/2$), and a constant, respectively. An estimation of band gap was acquired by extrapolation using tangent lines on the plot of $(\alpha h\nu)^{1/n}$ versus $h\nu$ and is shown in Figure 3(b). The results indicate that the band gap energies of Cu_1N_1, Cu_1N_2, and Cu_1N_3 codoped TiO_2 are 2.55 eV, 2.65 eV, and 2.90 eV, respectively. These band gaps are smaller than the widely accepted band gap values (3.2 eV and 3.0 eV) for pure TiO_2 and Degussa P25. The band structure of the photocatalysts played a crucial role in determining catalytic activity.

3.3. Morphology of the TiO_2 Films. Figure 5 shows the FE-SEM images of the oxide film surfaces formed by anodic oxidation treatment. Amorphously shaped oxide films were observed on the TiO_2 (Figures 5(a) and 5(b)) and after (Figures 5(c) and 5(d)) Cu/N codoping on TiO_2 films. The films were amorphous before codoping. It is obvious that the TiO_2 particles were successfully oxidized on titanium (Figures 5(c) and 5(d)).

Based on the SEM images, it was estimated that the TiO_2 film formed on the Ti substrate had a thickness film and the TiO_2 particle size was around 50 nm (Figure 5). Most parts of the TiO_2 film displayed a less porous surface (Figure 5(a)). With respect to Cu/N codoped TiO_2 film, a number of larger Cu grains, compared with TiO_2 particulates, were obviously observed (Figure 5(d)). In addition, the size of Cu grain increased rapidly with prolonging the illumination time. The N doped in TiO_2 was small in size and mainly filled in the gaps between TiO_2 particulates.

3.4. EDX Analysis. The EDX analysis was carried out to study the components of the deposited films (Figure 6). The result shows that these samples contain Ti substrate elements (Ti, O, and C) as well as Cu, confirming that Cu^{2+} is doped into the TiO_2 films. Further observation indicates that with increasing the concentration of Cu^{2+} in the deposition, the atom content of Cu element in the film is homologous augment (insets of Figures 6(a) and 6(b)). The actual percentage value of Cu in Cu_2N_3 codoped TiO_2 film is 3.14%. No nitrogen peaks were detected, presumably due to the fact that the content of N doping was very low and the doped N was uniformly distributed into the TiO_2 films.

3.5. Photocatalytic Activity of Cu/N Codoped TiO_2 Films. The visible light photocatalytic (PC) degradation of humic acid over the Cu/N TiO_2/Ti films, doped with different Cu^{2+}/NH_4^+ molar ratios codoped TiO_2, was evaluated. The results indicate that all Cu/N codoped TiO_2 films have PC activity toward the degradation of HA. In contrast, unmodified TiO_2 film was not effective in degrading HA, regardless

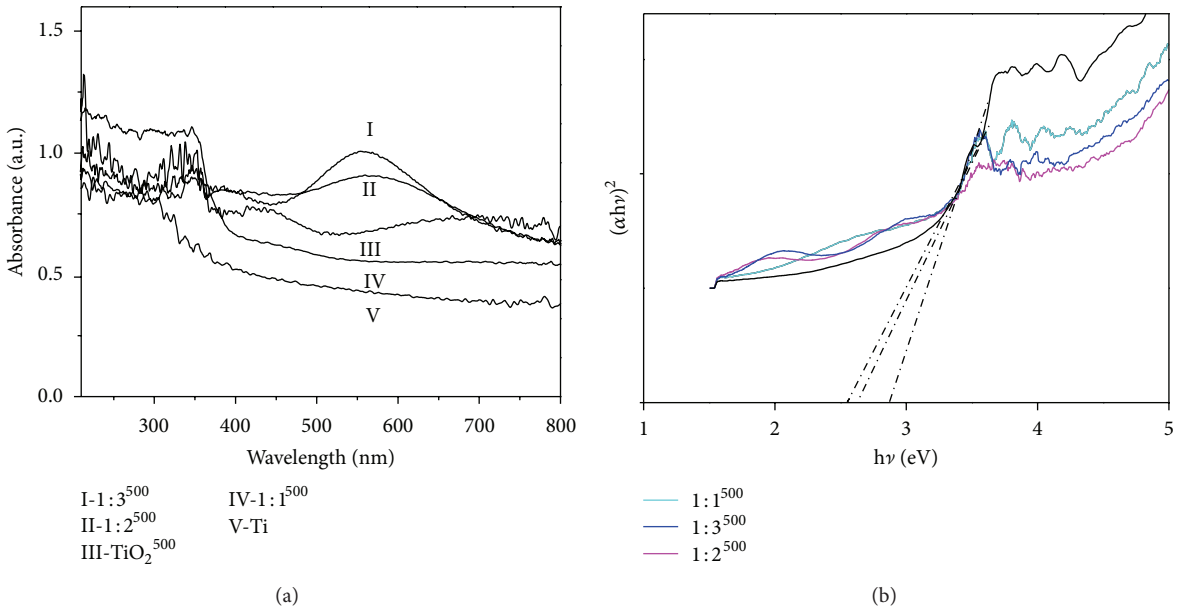

Figure 4: (a) UV-Vis DRS spectra for Ti, TiO_2-500, and codoped TiO_2-500 plate electrode and the corresponding plot of transformed Kubelka-Munk versus energy of light for TiO_2-500 and codoped TiO_2-500.

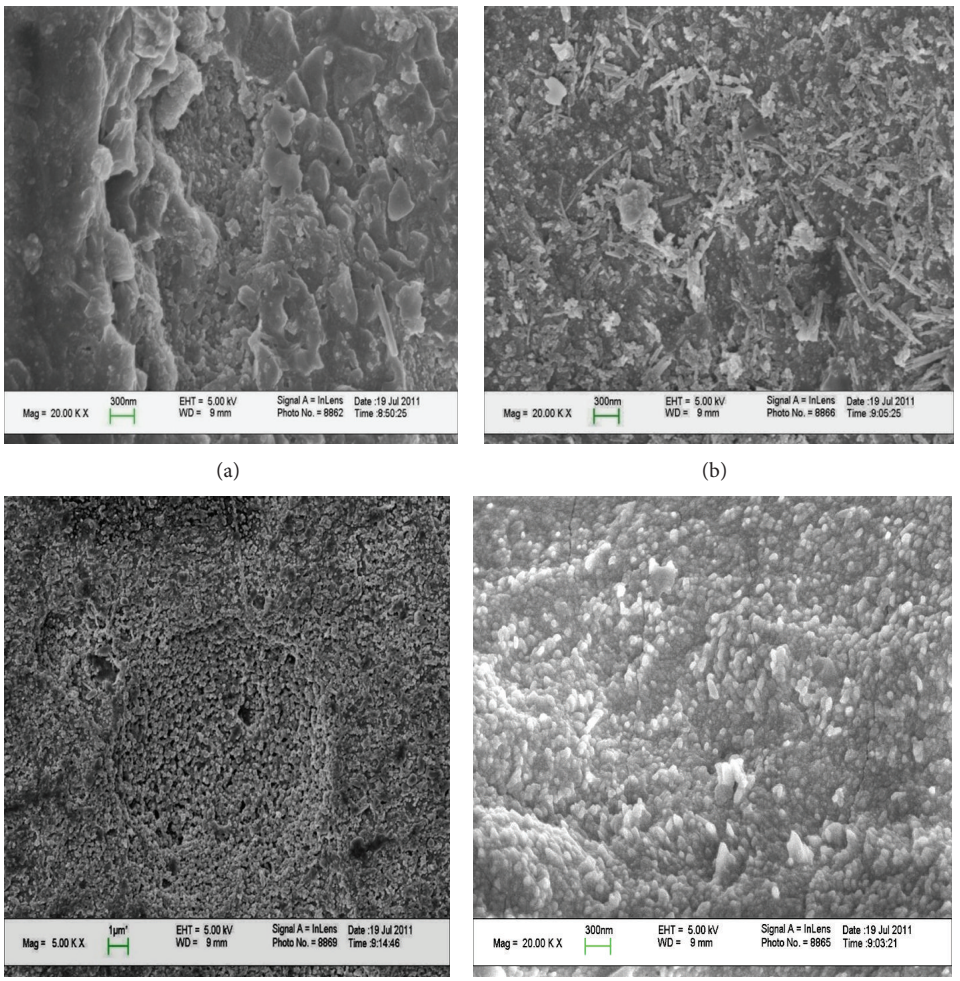

Figure 5: FESEM images of ((a) and (b)) view of pure TiO_2 film and ((c) and (d)) top view of Cu/N codoped TiO_2 film.

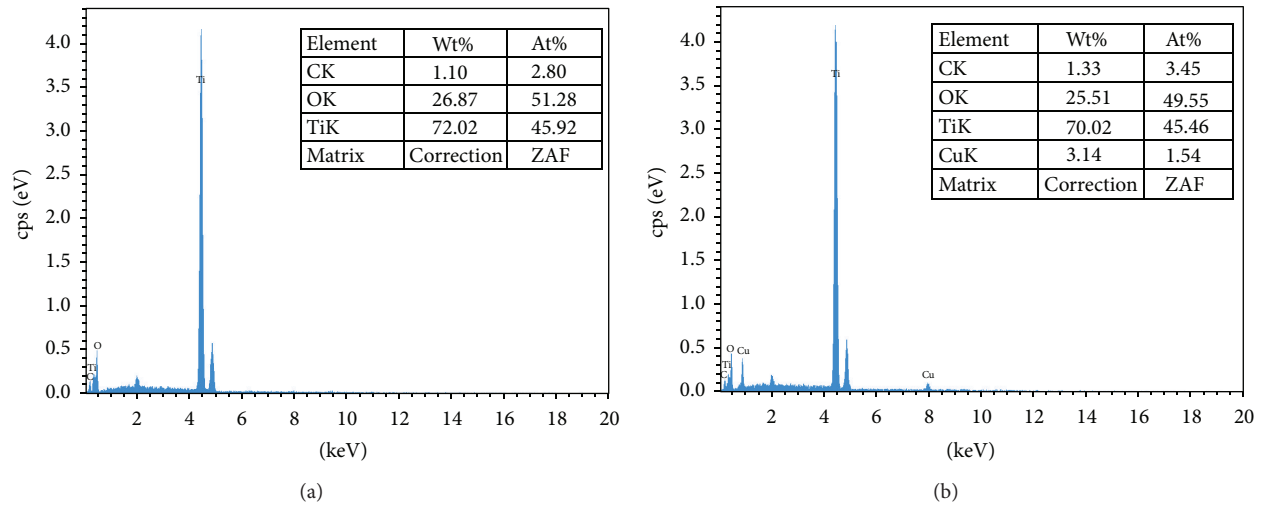

Figure 6: EDX spectra of (a) TiO_2 and (b) Cu_2N_3-TiO_2. The insets in (a) and (b) show the element analysis of composites.

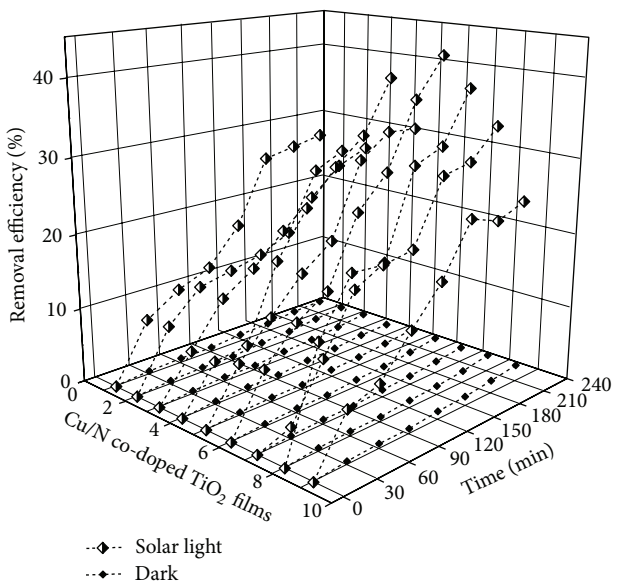

Figure 7: Degradation of humic acid under solar light and dark reaction over all Cu/N codoped TiO_2: (1) 1 : 1-500, (2) 1 : 2-500, (3) 1 : 3-500, (4) 2 : 1-500, (5) 2 : 2-500, (6) 2 : 3-500, (7) 3 : 1-500, (8) 3 : 2-500, and (9) 3 : 3-500.

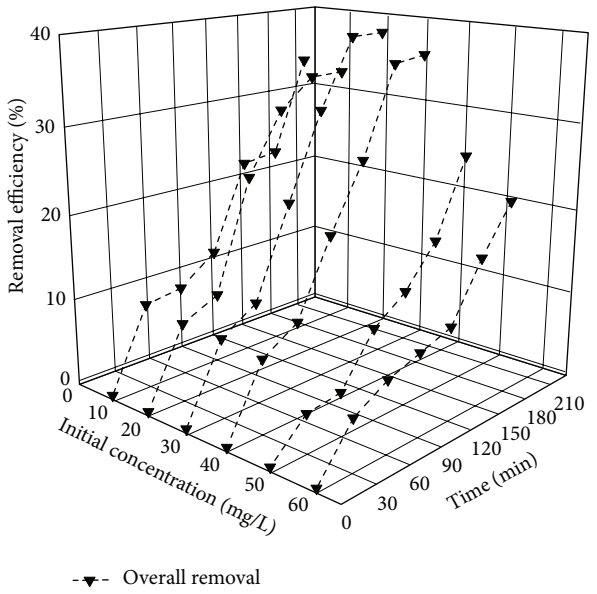

Figure 8: Removal efficiency curves of humic acid over 2 : 3 Cu/N codoped TiO_2 film by photocatalysis.

of illumination with strong light intensity. The highest PC degradation efficiency was achieved on the $Cu^{2+}/NH_4{}^+$ molar ratio 2 : 3 TiO_2 film (Figure 7). For instance, after 210 min of treatment, the $Cu^{2+}/NH_4{}^+$ molar ratio 2 : 3 Cu/N codoped TiO_2 film shows about 41.5% PC degradation efficiency when there only has illumination. Upon illumination with photon energy in the excess of the band gap energy (E_g < 3.2 eV) of the Cu/N codoped TiO_2 photocatalyst, photogenerated electrons can easily be generated under the visible light due to the $Cu^{2+}/NH_4{}^+$ ions doping. These photogenerated electrons take part in photocatalytic redox reactions. Previous research has shown that the hole reacts with the electron donors to produce free radical $OH^\bullet$ [38]. As the generation of free radical $OH^\bullet$, the humic acid decomposed into lower molecular weight compounds. When the Cu^{2+} content exceeded the optimum value (Cu_3N_x), the photocatalytic activity decreased. This result indicated that the presence of a greater amount of Cu was detrimental to the photocatalytic ability.

3.6. Effect of Initial Concentration of Humic Acid. The influence of the initial concentration of humic acid on the photocatalytic degradation is shown in Figure 8. The result indicates that the degradation efficiency is decreased with increasing the initial concentration of humic acid. It is likely that with high initial concentration of humic acid,

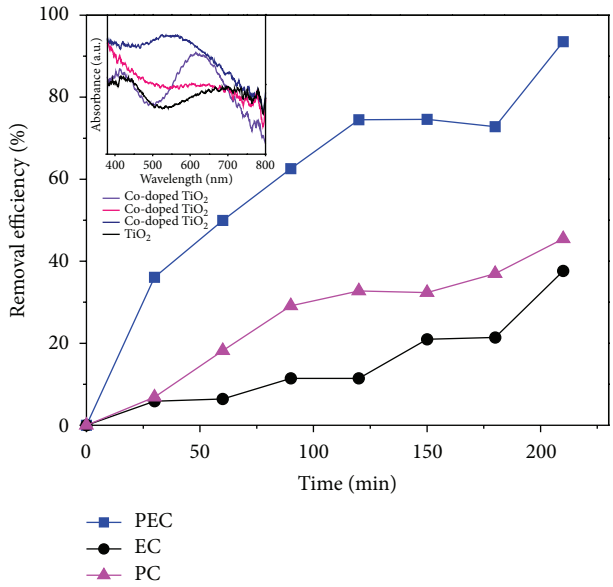

FIGURE 9: Photocatalysis, electrolysis, and photoelectrolysis removal efficiency of humic acid on 2 : 3 Cu/N codoped TiO_2 film.

an increased turbidity or cloudiness reduces the incident light and therefore reduces the activity. At the same time, adsorption of pollutant on photocatalyst plays an important role in removal of pollutant [50, 51]. Although the same amount of humic acid may be removed via adsorption until all the adsorption sites are occupied, the degradation efficiency based on $(C_0 - C)/C_0$ may be reduced at high initial concentration C_0.

3.7. Photocatalysis, Electrolysis, and Photoelectrocatalysis of Humic Acid. The visible light photocatalysis (PC), electrolysis (EC), and photoelectrocatalysis (PEC) activity of the Cu/N codoped TiO_2 films were evaluated for the degradation of humic acid in aqueous solution. The experimental results in Figure 9 showed that, compared with the PC oxidation, the PEC experiment was significantly higher than that of the PC process. For example, the Cu/N codoped TiO_2 film with molar ratio of 2 : 3 achieved UV254 removal efficiency of 93.5% in the PEC process, while it was only 41.5% in the PC process. The enhancement of UV-HA removal efficiency in the PEC processes can be ascribed to the following: the externally applied anodic bias drives away the photogenerated electrons accumulated on TiO_2 films via the external circuit, thus reducing the recombination of photogenerated electrons and holes and promoting the oxidation efficiency of humic acid. Figure 9 also showed that compared with the PC and PEC oxidation, EC oxidation was significantly decreased to only 37.6%.

The visible light sensitivity of the TiO_2 films caused by N doping (either substitutional or interstitial) may be related to the formation of high-energy level of steady state, which shifts the band-to-band electron transition to steady state to the conduction band transition. In the interstitial N model, the nitrogen atoms are bound to one or more oxygen atoms and therefore are in a positive oxidation state, which could be NO^-, NO_2^-, or NO_3^-. Unpaired electrons distribute around both N and O atoms in nitrogen oxides.

The energy level formed by nitrogen oxides has a π-bond feature. The two bonding orbital energy levels lie below the top of the O 2p band, while the two antibonding orbital energy levels lie above the O 2p band. The highest steady state level for the interstitial species is 0.73 eV above the top of the valence band. Excitation from these steady state high-energy levels to the conduction band is responsible for the shift of the optical absorption of pure TiO_2 toward the lower energies (in the visible region) [34]. Furthermore, Cu doping is helpful for enhancing the separation between photoinduced electrons and holes. As a result, the Cu/N codoping not only improves photocatalytic activities of TiO_2 films, but also extends their absorbance band to visible light region.

4. Conclusion

In summary, this work improved the facile electrochemical technique for preparing a series of Cu/N codoped TiO_2 films to study the effective degradation of humic acid under visible light. The Cu/N codoped TiO_2 films were successfully fabricated. The absorption wavelength range and visible light photocatalytic activity of as-prepared Cu/N-codoped TiO_2 films were obviously affected by different molar ratios of Cu^{2+}/NH_4^+. The doping with suitable amounts of nitrogen and Cu into TiO_2 films exhibited a synergistic effect on the improvement of the photocatalytic efficiency of TiO_2 in visible light regions. Using the molar ratio 2 : 3 Cu/N TiO_2 film, the PEC degradation efficiency of humic acid under visible light illumination reached 93.5% after 210 min of treatment. Our work demonstrates that anodic oxidation technique is useful for preparing metal and nonmetal ion-doped TiO_2 films for visible light PEC degradation of organic pollutants.

Conflict of Interests

The authors declare that they have no conflict of interests regarding the publication of this paper.

Acknowledgments

The authors wish to thank the State Ministry of Science and Technology (2008BAE64B05), the National Natural Science Foundation (21277052), the State Key Laboratory of Subtropical Building Science (2011ZB05, 2012ZB06, and 2013ZC03), the Department of Science and Technology of Guangdong Province (2007A032500005), the Department of Guangdong Education and the Science and Technology Bureau (2008A1-D0011), and the Environmental Protection Bureau (201203) for their financial support. In addition, the kind suggestions from the anonymous reviewers are greatly acknowledged.

References

[1] W. J. Weber Jr., Q. Huang, and R. A. Pinto, "Reduction of disinfection byproduct formation by molecular reconfiguration of the fulvic constituents of natural background organic matter,"

Environmental Science and Technology, vol. 39, no. 17, pp. 6446–6452, 2005.

[2] R. L. Wershaw, "Humus chemistry: genesis, composition, reactions: by F. J. Stevenson. Wiley-Interscience, New York, 1982, xiii + 443 pp," *Organic Geochemistry*, vol. 4, no. 3-4, 223 pages, 1983.

[3] F. J. Stevenson, *Humus Chemistry: Genesis, Composition, Reactions*, Wiley, New York, NY, USA, 1982.

[4] M. Aeschbacher, S. H. Brunner, R. P. Schwarzenbach, and M. Sander, "Assessing the effect of humic acid redox state on organic pollutant sorption by combined electrochemical reduction and sorption experiments," *Environmental Science and Technology*, vol. 46, no. 7, pp. 3882–3890, 2012.

[5] Y. Nagata, K. Hirai, H. Bandow, and Y. Kimaeda, "Decomposition of hydroxybenzoic and humic acids in water by ultrasonic irradiation," *Environmental Science and Technology*, vol. 30, no. 4, pp. 1133–1138, 1996.

[6] K. Tanaka and K. S. N. Reddy, "Photodegradation of phenoxyacetic acid and carbamate pesticides on TiO_2," *Applied Catalysis B*, vol. 39, no. 4, pp. 305–310, 2002.

[7] R. Zhang, L. Gao, and Q. Zhang, "Photodegradation of surfactants on the nanosized TiO_2 prepared by hydrolysis of the alkoxide titanium," *Chemosphere*, vol. 54, no. 3, pp. 405–411, 2004.

[8] B. Yu, J. Zeng, L. Gong, M. Zhang, L. Zhang, and X. Chen, "Investigation of the photocatalytic degradation of organochlorine pesticides on a nano-TiO_2 coated film," *Talanta*, vol. 72, no. 5, pp. 1667–1674, 2007.

[9] D. Dong, P. Li, X. Li et al., "Photocatalytic degradation of phenanthrene and pyrene on soil surfaces in the presence of nanometer rutile TiO_2 under UV-irradiation," *Chemical Engineering Journal*, vol. 158, no. 3, pp. 378–383, 2010.

[10] A. Kaur and U. Gupta, "A review on applications of nanoparticles for the preconcentration of environmental pollutants," *Journal of Materials Chemistry*, vol. 19, no. 44, pp. 8279–8289, 2009.

[11] S. Anandan, Y. Ikuma, and K. Niwa, "An overview of semiconductor photocatalysis: modification of TiO_2 nanomaterials," *Diffusion and Defect Data B*, vol. 162, pp. 239–260, 2010.

[12] J. Li, J. Wang, L. Huang, and G. Lu, "Photoelectrocatalytic degradation of methyl orange over mesoporous film electrodes," *Photochemical and Photobiological Sciences*, vol. 9, no. 1, pp. 39–46, 2010.

[13] S. Yin, Q. Zhang, F. Saito, and T. Sato, "Preparation of visible light-activated titania photocatalyst by mechanochemical method," *Chemistry Letters*, vol. 32, no. 4, pp. 358–359, 2003.

[14] A. Ghicov, B. Schmidt, J. Kunze, and P. Schmuki, "Photoresponse in the visible range from Cr doped TiO_2 nanotubes," *Chemical Physics Letters*, vol. 433, no. 4–6, pp. 323–326, 2007.

[15] D. Li, H. Huang, X. Chen et al., "New synthesis of excellent visible-light $TiO_{2-x}N_x$ photocatalyst using a very simple method," *Journal of Solid State Chemistry*, vol. 180, no. 9, pp. 2630–2634, 2007.

[16] E. D. B. Santos, J. M. De Souza E Silva, F. A. Sigoli, and I. O. Mazali, "Size-controllable synthesis of functional heterostructured TiO_2-WO_3 core-shell nanoparticles," *Journal of Nanoparticle Research*, vol. 13, no. 11, pp. 5909–5917, 2011.

[17] F. Chen, Z. Deng, X. Li, J. Zhang, and J. Zhao, "Visible light detoxification by 2,9,16,23-tetracarboxyl phthalocyanine copper modified amorphous titania," *Chemical Physics Letters*, vol. 415, no. 1–3, pp. 85–88, 2005.

[18] H.-C. Liang and X.-Z. Li, "Visible-induced photocatalytic reactivity of polymer-sensitized titania nanotube films," *Applied Catalysis B*, vol. 86, no. 1-2, pp. 8–17, 2009.

[19] A. Ghicov, B. Schmidt, J. Kunze, and P. Schmuki, "Photoresponse in thevisible range from Cr doped TiO_2 nanotubes," *Chemical Physics Letters*, vol. 433, no. 4–6, pp. 323–326, 2007.

[20] R. Asahi, T. Morikawa, T. Ohwaki, K. Aoki, and Y. Taga, "Visible-light photocatalysis in nitrogen-doped titanium oxides," *Science*, vol. 293, no. 5528, pp. 269–271, 2001.

[21] A. W. Morawski, M. Janus, B. Tryba, M. Inagaki, and K. Kałucki, "TiO_2-anatase modified by carbon as the photocatalyst under visible light," *Comptes Rendus Chimie*, vol. 9, no. 5-6, pp. 800–805, 2006.

[22] T. Ohno, N. Murakami, T. Tsubota, and H. Nishimura, "Development of metal cation compound-loaded S-doped TiO_2 photocatalysts having a rutile phase under visible light," *Applied Catalysis A*, vol. 349, no. 1-2, pp. 70–75, 2008.

[23] Y. Shen, T. Xiong, T. Li, and K. Yang, "Tungsten and nitrogen codoped TiO_2 nano-powders with strong visible light response," *Applied Catalysis B*, vol. 83, no. 3-4, pp. 177–185, 2008.

[24] W. Y. Teoh, R. Amal, L. Mädler, and S. E. Pratsinis, "Flame sprayed visible light-active Fe-TiO_2 for photomineralisation of oxalic acid," *Catalysis Today*, vol. 120, no. 2, pp. 203–213, 2007.

[25] G. Tian, K. Pan, H. Fu, L. Jing, and W. Zhou, "Enhanced photocatalytic activity of S-doped TiO_2-ZrO_2 nanoparticles under visible-light irradiation," *Journal of Hazardous Materials*, vol. 166, no. 2-3, pp. 939–944, 2009.

[26] L. Li, C.-Y. Liu, and Y. Liu, "Study on activities of vanadium (IV/V) doped TiO_2(R) nanorods induced by UV and visible light," *Materials Chemistry and Physics*, vol. 113, no. 2-3, pp. 551–557, 2009.

[27] A. Kubacka, G. Colón, and M. Fernández-García, "Cationic (V, Mo, Nb, W) doping of TiO_2-anatase: a real alternative for visible light-driven photocatalysts," *Catalysis Today*, vol. 143, no. 3-4, pp. 286–292, 2009.

[28] E. B. Gracien, J. Shen, X. Sun et al., "Photocatalytic activity of manganese, chromium and cobalt-doped anatase titanium dioxide nanoporous electrodes produced by re-anodization method," *Thin Solid Films*, vol. 515, no. 13, pp. 5287–5297, 2007.

[29] J. Zhao, X. Wang, R. Chen, and L. Li, "Fabrication of titanium oxide nanotube arrays by anodic oxidation," *Solid State Communications*, vol. 134, no. 10, pp. 705–710, 2005.

[30] S. Kaneco, Y. Chen, P. Westerhoff, and J. C. Crittenden, "Fabrication of uniform size titanium oxide nanotubes: impact of current density and solution conditions," *Scripta Materialia*, vol. 56, no. 5, pp. 373–376, 2007.

[31] M. Anpo, S. Dohshi, M. Kitano, Y. Hu, M. Takeuchi, and M. Matsuoka, "The preparation and characterization of highly efficient titanium oxide-based photofunctional materials," *Annual Review of Materials Research*, vol. 35, pp. 1–27, 2005.

[32] C. E. Schvezov, M. A. Alterach, M. L. Vera, M. R. Rosenberger, and A. E. Ares, "Characteristics of hemocompatible TiO_2 nanofilms produced by the sol-gel and anodic oxidation techniques," *JOM*, vol. 62, no. 6, pp. 84–87, 2010.

[33] K. Vinodgopal, S. Hotchandani, and P. V. Kamat, "Electrochemically assisted photocatalysis: titania particulate film electrodes for photocatalytic degradation of 4-chlorophenol," *The Journal of Physical Chemistry*, vol. 97, no. 35, pp. 9040–9044, 1993.

[34] D. Dumitriu, A. R. Bally, C. Ballif et al., "Photocatalytic degradation of phenol by TiO_2 thin films prepared by sputtering," *Applied Catalysis B*, vol. 25, no. 2-3, pp. 83–92, 2000.

[35] X. Quan, X. Ruan, H. Zhao, S. Chen, and Y. Zhao, "Photoelectrocatalytic degradation of pentachlorophenol in aqueous solution using a TiO_2 nanotube film electrode," *Environmental Pollution*, vol. 147, no. 2, pp. 409–414, 2007.

[36] Y. Xu, J. Jia, D. Zhong, and Y. Wang, "Degradation of dye wastewater in a thin-film photoelectrocatalytic (PEC) reactor with slant-placed TiO_2/Ti anode," *Chemical Engineering Journal*, vol. 150, no. 2-3, pp. 302–307, 2009.

[37] J. Zhang, B. Zhou, Q. Zheng et al., "Photoelectrocatalytic COD determination method using highly ordered TiO_2 nanotube array," *Water Research*, vol. 43, no. 7, pp. 1986–1992, 2009.

[38] J. Yang, J. Dai, C. Chen, and J. Zhao, "Effects of hydroxyl radicals and oxygen species on the 4-chlorophenol degradation by photoelectrocatalytic reactions with TiO_2-film electrodes," *Journal of Photochemistry and Photobiology A*, vol. 208, no. 1, pp. 66–77, 2009.

[39] K. Esquivel, L. G. Arriaga, F. J. Rodríguez, L. Martínez, and L. A. Godínez, "Development of a TiO_2 modified optical fiber electrode and its incorporation into a photoelectrochemical reactor for wastewater treatment," *Water Research*, vol. 43, no. 14, pp. 3593–3603, 2009.

[40] A. Fujishima, T. N. Rao, and D. A. Tryk, "Titanium dioxide photocatalysis," *Journal of Photochemistry and Photobiology C*, vol. 1, no. 1, pp. 1–21, 2000.

[41] R. Daghrir, P. Drogui, and D. Robert, "Photoelectrocatalytic technologies for environmental applications," *Journal of Photochemistry and Photobiology A*, vol. 238, pp. 41–52, 2012.

[42] Y. Su, S. Han, X. Zhang, X. Chen, and L. Lei, "Preparation and visible-light-driven photoelectrocatalytic properties of boron-doped TiO_2 nanotubes," *Materials Chemistry and Physics*, vol. 110, no. 2-3, pp. 239–246, 2008.

[43] X. Wang, H. Zhao, X. Quan, Y. Zhao, and S. Chen, "Visible light photoelectrocatalysis with salicylic acid-modified TiO_2 nanotube array electrode for p-nitrophenol degradation," *Journal of Hazardous Materials*, vol. 166, no. 1, pp. 547–552, 2009.

[44] B. S. Liu, L. P. Wen, and X. J. Zhao, "Efficient degradation of aqueous methyl orange over TiO_2 and CdS electrodes using photoelectrocatalysis under UV and visible light irradiation," *Progress in Organic Coatings*, vol. 64, no. 2-3, pp. 120–123, 2009.

[45] S. Park and T.-I. Yoon, "The effects of iron species and mineral particles on advanced oxidation processes for the removal of humic acids," *Desalination*, vol. 208, no. 1–3, pp. 181–191, 2007.

[46] W.-C. Hung, Y.-C. Chen, H. Chu, and T.-K. Tseng, "Synthesis and characterization of TiO_2 and Fe/TiO_2 nanoparticles and their performance for photocatalytic degradation of 1,2-dichloroethane," *Applied Surface Science*, vol. 255, no. 5, pp. 2205–2213, 2008.

[47] C. Kim, J. T. Kim, K. S. Kim, S. Jeong, H. Y. Kim, and Y. S. Han, "Immobilization of TiO_2 on an ITO substrate to facilitate the photoelectrochemical degradation of an organic dye pollutant," *Electrochimica Acta*, vol. 54, no. 24, pp. 5715–5720, 2009.

[48] S. Xu, J. Ng, X. Zhang, H. Bai, and D. D. Sun, "Fabrication and comparison of highly efficient Cu incorporated TiO_2 photocatalyst for hydrogen generation from water," *International Journal of Hydrogen Energy*, vol. 35, no. 11, pp. 5254–5261, 2010.

[49] L. Yiming, L. Wei, Z. Wanggang, Z. Jianjun, and H. Peide, "First principle study of Cu-N, Cu and N-doped anatase TiO_2 ," *Solid State Communications*, vol. 164, pp. 27–31, 2013.

[50] S. Saepurahman, M. A. Abdullah, and F. K. Chong, "Dual-effects of adsorption and photodegradation of methylene blue by tungsten-loaded titanium dioxide," *Chemical Engineering Journal*, vol. 158, no. 3, pp. 418–425, 2010.

[51] S. Bekkouche, M. Bouhelassa, N. Hadj Salah, and F. Z. Meghlaoui, "Study of adsorption of phenol on titanium oxide (TiO_2)," *Desalination*, vol. 166, no. 1–3, pp. 355–362, 2004.